

Thermal design of power transformers via CFD

Ralf Wittmaack

Siemens E T TR LPT PN GTC LPT R&D, Katzwanger Str. 150, 90461 Nürnberg, Germany
Ralf.Wittmaack@Siemens.com

Key Words: *CFD, Power Transformers, Radiant Heat Transfer.*

ABSTRACT

At Siemens, an in-house CFD code UniFlow is used to investigate fluid flow and heat transfer in oil-immersed and dry-type transformers, as well as transformer components like windings, cores, tank walls, and radiators. This paper outlines its physical models and numerical solution methods.

Moreover, for oil-immersed transformers, it presents an application to a high voltage (HV) winding in a traction transformer of locomotives, cooled by synthetic ester. In this case the goal is to find the maximum temperatures in the insulation materials.

Furthermore, as a dry-type transformer application, an air cooled cast resin transformer prototype operated at ships in an enclosure is investigated. For this application, the ventilator driven air flow is cooled by sea water. In addition to the low and high voltage windings, the core is also a part of the simulation. In this case, the radiation makes a significant contribution to the heat transfer.

1 INTRODUCTION

The life time of power transformers is substantially influenced by chemical degradation processes occurring in the electrical insulation. Since the speed of these processes depends significantly on temperature, the proper prediction of component temperatures during transformer operation is a crucial part of the design process. There are several sources of heat in the transformer. If a time varying voltage is applied, in the steel sheets of the core, magnetic hysteresis effects and eddy currents lead to no-load losses. In addition, during normal operation the electrical currents cause Ohmic and stray load losses.

To keep the temperatures of the transformer components within acceptable limits, appropriate cooling is quintessential. Depending on the type of transformer, this is normally accomplished via natural or forced convection of the cooling fluids air or oil. In addition to mineral and silicone oil also natural and synthetic ester fluids are used.

Thanks to its flexibility and accuracy, CFD (Computational Fluid Dynamics) is increasingly being used to analyse transformer thermal design. This follows the trend established in other branches of advanced technology development like aerospace, automotive, and power generation, where CFD simulations are indispensable parts of the product development cycles.

Employing commercial CFD codes, several detailed studies of disc-type transformer windings were performed, e.g., by Torriano, Chaaban, and Pichler [1]. Moreover, extended full geometry CFD analyses coupled to electromagnetic simulation of the load and no-load losses in core and windings were presented, e.g., by Smolka and Nowak [2], [3]. Furthermore, combined oil and air flows in fin-type distribution transformers were investigated with commercial CFD codes, e.g., by [4], [5].

Our intention is to provide a simulation method that may be used for detailed CFD analyses on fine grids as well as for simplified coarse grid studies. The in-house code UniFlow is designed to be

applicable also by users with limited experience in CFD. For this reason, e.g., material attributes are employed for a convenient coupling of fluid and solid regions in conjugate heat transfer simulations.

2 PHYSICAL MODELS AND NUMERICAL METHODS

2.1 Physical models

Our physical model is aimed at investigating flows with several kinds of heat transfer in a complex geometry. It simulates the flow of single-component, incompressible Newtonian fluids in a three-dimensional geometry. In addition to the fluids, in gaseous or liquid state, several structural materials are considered as hydrodynamic obstacles and thermodynamic heat structures. The hydrodynamics is described by the continuity equation and the Navier-Stokes equation. For the simulation of turbulence the algebraic Baldwin-Lomax eddy viscosity model is available. To simulate the transition between laminar and turbulent flows, algebraic transition models of Drela and Mayle are on hand.

For temperature dependent density or material properties of the viscous stress tensor, the hydrodynamics of the fluid is coupled to the thermodynamics. For this reason, internal heat transfer (by convection and conduction) and heat generation by internal sources as well as heat transfer to the surroundings are modelled via a heat transport equation. To allow for the simulation of phase transitions it is provided in enthalpy formulation. At the rigid boundaries heat conduction is considered. For coarse grids convective heat transfer coefficients may be employed at solid-liquid interfaces. Radiant heat transfer is simulated at structural material surfaces. The material properties (density, dynamic viscosity, specific heat, heat conductivity, and convective heat transfer coefficient) depend on the temperature. Solids may have orthotropic heat conductivity.

2.1.1 Dynamic equations

Our dynamic equations are written in Cartesian coordinates. The continuity equation for incompressible flow is [6]

$$\frac{\partial}{\partial x^m} (\rho v^m) = 0 \quad ,$$

where ρ is density and v velocity. x are the space coordinates and we use Einstein's summation convention for the space direction index m . Introduction of the continuity equation into the Navier-Stokes equation [6] leads to a momentum equation in strong conservation form

$$\rho \frac{\partial v_i}{\partial t} + \frac{\partial}{\partial x^m} \left[\rho v_i v^m - \mu \left(\frac{\partial v_i}{\partial x_m} + \frac{\partial v^m}{\partial x^i} \right) \right] = - \frac{\partial p}{\partial x^i} + \rho g_i \quad ,$$

where t is time, p pressure, and g gravitational acceleration. After inclusion of the continuity equation our heat transport equation in strong conservation form reads

$$\rho \frac{\partial h}{\partial t} + \frac{\partial}{\partial x^m} \left(\rho h v^m - \lambda \frac{\partial T}{\partial x_m} \right) = P_d \quad .$$

Here h is specific enthalpy, T temperature, λ heat conductivity, and P_d density of the heat sources or sinks.

2.1.2 Radiant heat transfer model

Radiant heat transfer may be simulated between structural material surfaces adjacent to the fluid. The employed radiation model assumes that the radiating surfaces are boundaries of a hollow space with linear dimension much greater than their distance. It is applicable for, e.g., parallel plates and concentric cylinders. With this simplifying assumption the power received by surface 'a' via the heat transfer from surface 'b' is [7]

$$P_{ab} = c_{ab} A_a (T_b^4 - T_a^4) \quad ; \quad c_{ab} := \frac{\sigma}{\frac{1}{\varepsilon_a} + \frac{A_a}{A_b} \left(\frac{1}{\varepsilon_b} - 1 \right)} .$$

Here A is area of a radiating structural material surface, T surface temperature, $\sigma=5.67051 \cdot 10^{-8}$ W/(m²K⁴) Stefan-Boltzmann constant, and ε emissivity of a structural material surface. Computation domain nodes undergoing radiant heat transfer may have their radiation partner nodes inside the computation domain or at the boundary.

2.2 Numerical methods

For the numerical representation of our model we developed a finite volume method and employ boundary fitted, curvilinear, non-orthogonal, block-structured grids. The blocks may be connected via 1-to-1 or patched couplings. The arrangement of the dynamic variables in the control volumes of the grid is collocated at the node centre. The dynamic equations are solved sequentially. For the solution of the momentum, pressure-correction, and heat transport equations we use implicit schemes. The system of continuity and momentum equations is solved by a SIMPLE [8], SIMPLEC [9], or PISO [10] algorithm.

To speed up the code execution and to simplify the estimation of discretisation errors a FAS multi-grid algorithm is employed [11]. It is a geometric approach with standard coarsening applied to the outer iterations, visiting the grid levels in V-cycles. For steady-state problems it operates as a full multi-grid algorithm (FMG), whereas for transient problems the algorithm starts at the finest grid.

For the efficient solution of sparse linear equations several algorithms are available. The parabolic momentum and heat transport equations may be solved with a SIP solver that is modified to handle block couplings via the residual vector [8]. Additionally, for the elliptic pressure-correction equation an aggregation-based algebraic multi-grid algorithm [12] is available.

The UniFlow source code is written in C++. For multi-threaded shared memory parallelism, OpenMP is employed.

3 APPLICATIONS

Two transformer applications of the method are outlined, where we analyse one of the limbs. For the traction transformer we consider a 3-dimensional angular segment of the circumference. The simulations of the cast resin transformer are in a 2-dimensional cylindrical coordinate system with rectangular grids. Further on, geometrically more complex UniFlow calculations are described, e.g., in [13], while [14] describes thermal simulations of 5 windings of an oil transformer in a test bay.

In the applications outlined in this paper we analyse steady states. Furthermore, load losses are calculated by Maxwell-solvers and subsequently mapped to the CFD grids. Another common feature of the presented applications is that the active part is studied with prescribed fluid flow via in- and outlet boundary conditions, i.e., only parts of the entire coolant loops are considered.

3.1 Synthetic ester cooled traction transformer

For an application with synthetic ester cooling, we consider the HV winding in a traction transformer used in locomotives. In this application, the goal is to find the maximum temperatures in the insulation materials to allow for the selection of appropriate materials that withstand the thermal load.

The transformer has two wounded limbs that are located horizontally. Its outside view and the active part of a similar transformer are shown in the following figures. The outside view also shows the oil pump that is used for the directed oil flow. In our simulation the oil inlet occurs at the bottom of the windings, while the oil outlet is on top. At the inlet the average oil velocity is 0.9 m/s and the ester temperature is 364.55 K.

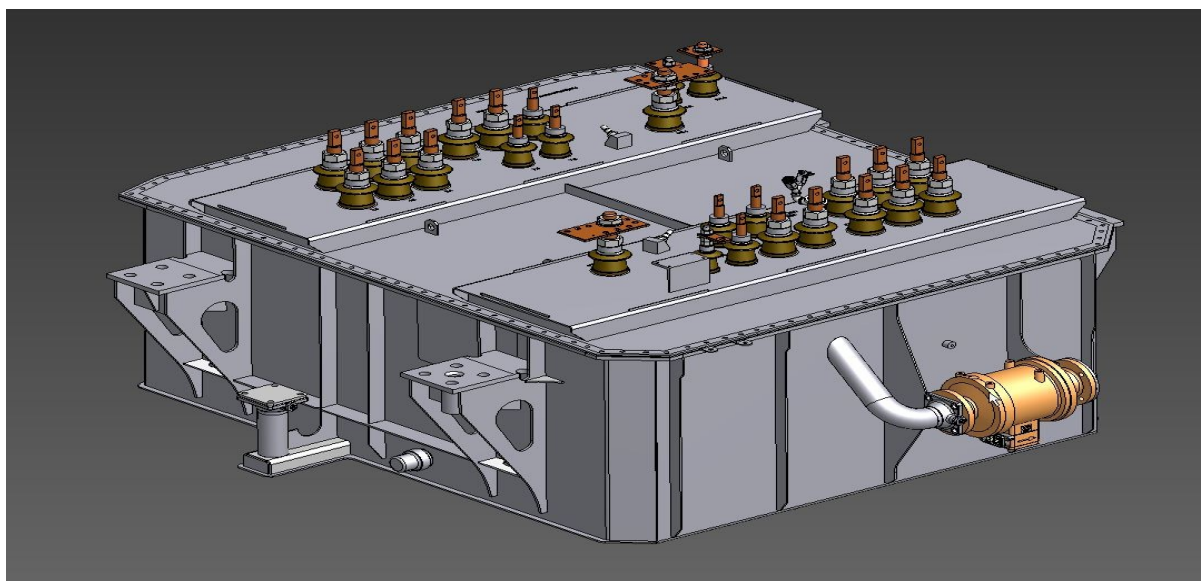


Figure 1a : Outside view of traction transformer

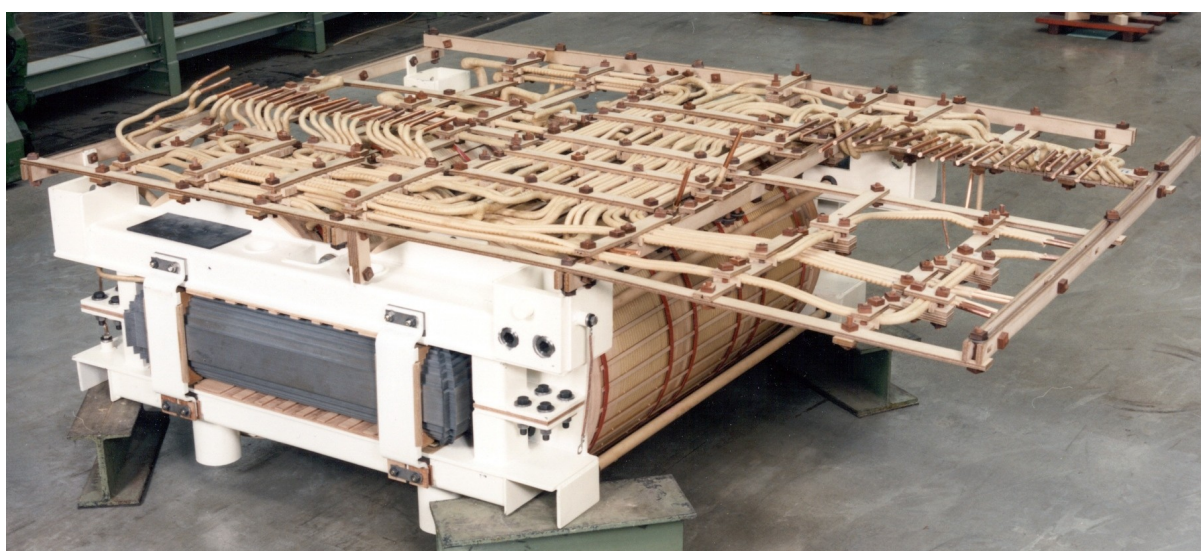


Figure 1b : Active part without tap changer

To indicate the location of the different materials, the two figures below show the initial specific enthalpy of an axial segment of the HV windings. Same as the entire geometry model of the simulation, it covers a periodical angular section of 7.5° of the circumference, corresponding to 24 spacers along the circumference. However, in the axial direction it represents only half a coil while the entire geometry model includes 92 coils. In this figure grey indicates ester, red pressboard, blue conductor, and light blue Nomex.

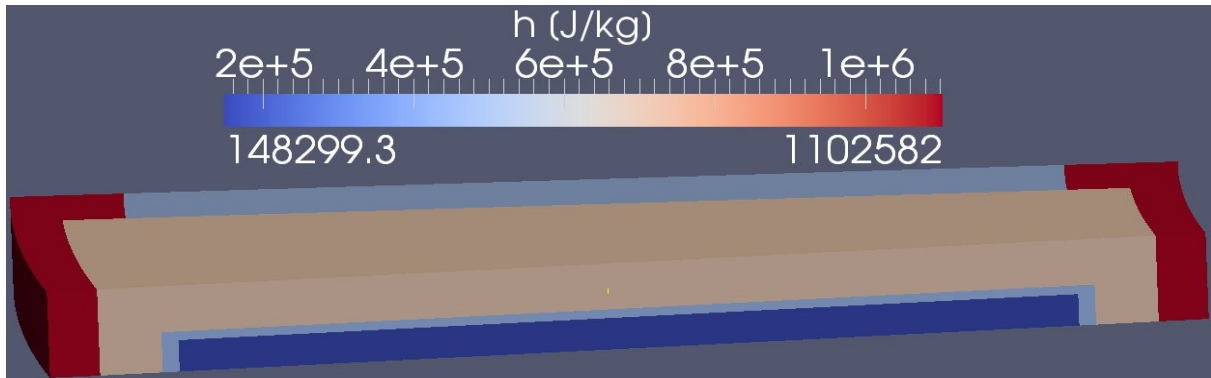


Figure 2a : Initial specific enthalpy of HV winding segment at ester side

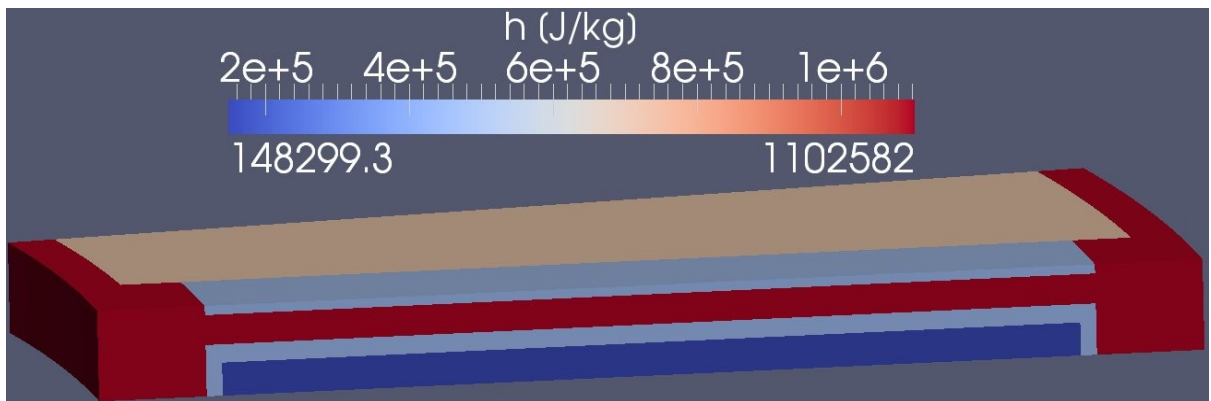


Figure 2b : Initial specific enthalpy of HV winding segment at spacer side

3.1.1 Spatial discretisation and boundary layer thickness

A single block grid with 706560 nodes is used, where 222880 nodes represent the ester while the rest corresponds to structural materials. Only 1 geometric multi-grid level is used since this for the many materials to be resolved in the computation domain leads to the most useful distribution of grid nodes. With the width of a winding segment l of 74.5 mm as characteristic length, the ester inlet velocity of 0.9 m/s, and the average ester temperature of 368 K, the Reynolds number R is 6875 and the Prandtl number Pr is 140. The ester flow along a winding segment resembles flow along a flat plate, where the transition from laminar to turbulent flow occurs between $R = 3.5 \cdot 10^5$ and 10^6 [15]. This indicates that the ester flow is laminar, i.e. the hydrodynamic and thermal boundary layer thickness may be estimated via [6]

$$\delta_h \sim \frac{l}{\sqrt{R}} \quad ; \quad \delta_t \sim \delta_h Pr^{-\frac{1}{3}} .$$

This leads to $\delta_h = 0.9$ mm and $\delta_t = 0.17$ mm at the end of a winding segment, i.e., the grid of our simulation of the traction transformer windings is too coarse to resolve the hydrodynamic and thermal boundary layers. To compensate for that, convective heat transfer coefficients are used at all interfaces of ester and structural materials. These were calculated via a detail model and a fine grid.

3.1.2 Material properties

Structural materials considered in this simulation are copper and its adjacent Nomex 410 isolation as well as pressboard and Nomex 994 isolation. In our grid the winding is split up into an inner and an outer part, made up of the copper conductor and Nomex 410. The inner part consists mainly of copper and includes only thin axial Nomex 410 layers. Their mixture material properties are calculated via

$$\rho_{mix} := \sum_{i=1}^{n_{mat}} \alpha_i \rho_i ; \quad c_{p,mix} := \sum_{i=1}^{n_{mat}} x_i c_{p,i} ; \quad \lambda_{mix} := \left(\sum_{i=1}^{n_{mat}} \frac{\alpha_i}{\lambda_i} \right)^{-1} ; \quad \alpha_i := \frac{V_i}{V} ; \quad x_i := \alpha_i \frac{\rho_i}{\rho_{mix}} .$$

Here α and x are volume fraction and mass fraction. To account for Nomex 410 in the inner winding region, we employ orthotropic heat conductivity. This reduces the heat conduction in the radial direction.

In our calculation temperature dependent material properties are used for ester and pressboard. Constant material properties at characteristic temperatures are listed in the following table.

Variable	Unit	Ester	Cu	Nomex 410	Inner HV	Outer HV	Nomex 994	Pressboard
α_{Cu}	-	-	-	-	0.95	0.6774	-	-
$\alpha_{Nomex\ 410}$	-	-	-	-	0.05	0.3226	-	-
ρ	kg/m ³	939	8930	720	8519.5	6281.45	1150	1210
μ	Pa s	0.31175	-	-	-	-	-	-
c_p	J/(kg K)	1789	382	1200	385.46	412.25	1200	3008
λ	W/(m K)	0.198	399	0.103	2.05 / 399	0.319	0.16	0.21

Table 1 : Material properties of traction transformer simulations

3.1.3 Simulation results

The following two figures show the radial and axial velocity components of the ester. They indicate the location of the axial flow barriers that lead to a meandering oil flow.

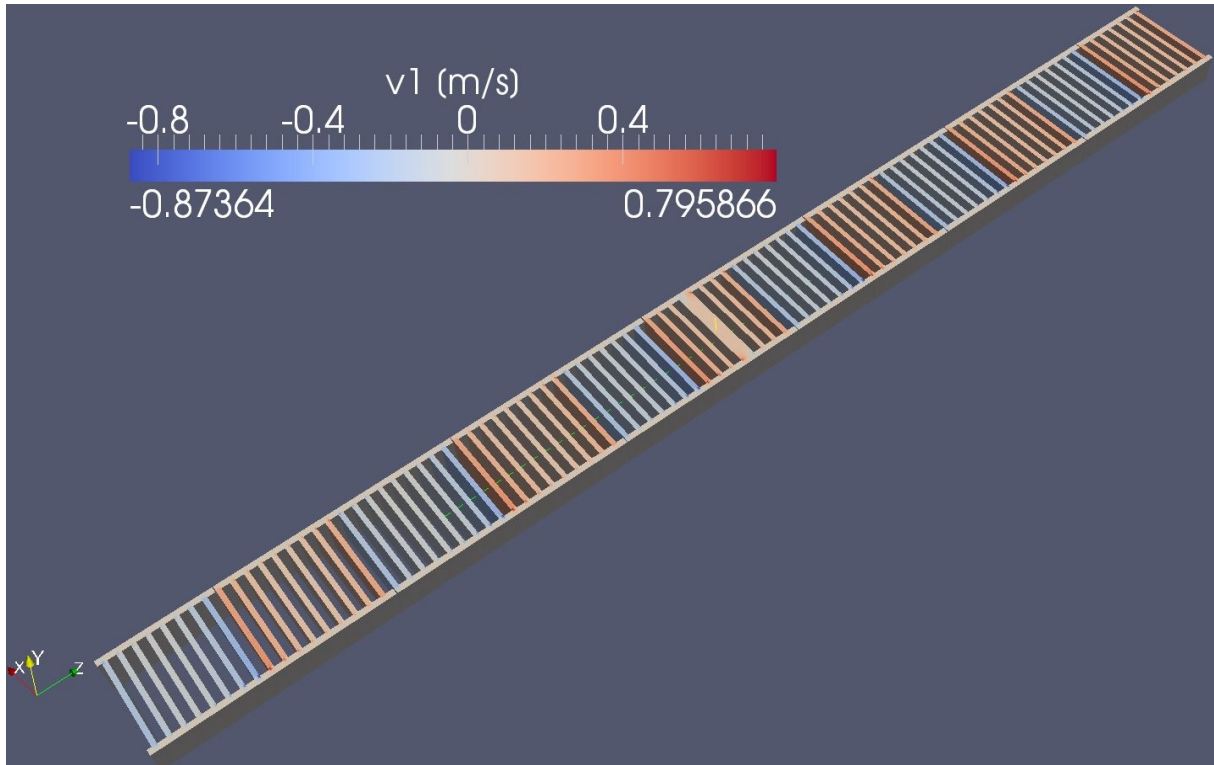


Figure 3 : Radial component of oil velocity in traction transformer winding

The maximum axial velocity is considerably higher than the inlet velocity. The maximum value occurs at the inner side, where the flow area is smaller.

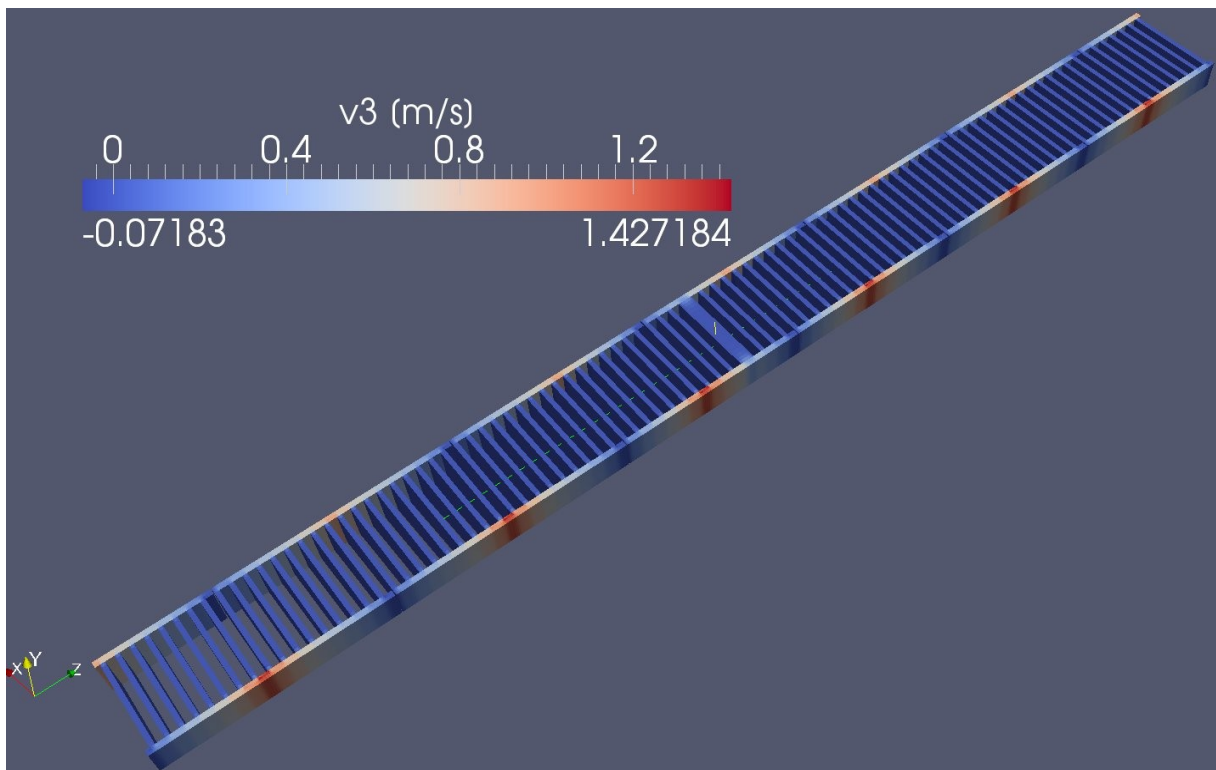


Figure 4 : Axial component of oil velocity in traction transformer winding

The next figure shows the calculated pressure in the ester. There is some stagnation pressure at the axial flow barriers. As the limbs are located horizontally we run our simulations without gravitational acceleration. For this reason there is no hydrostatic contribution to the pressure.

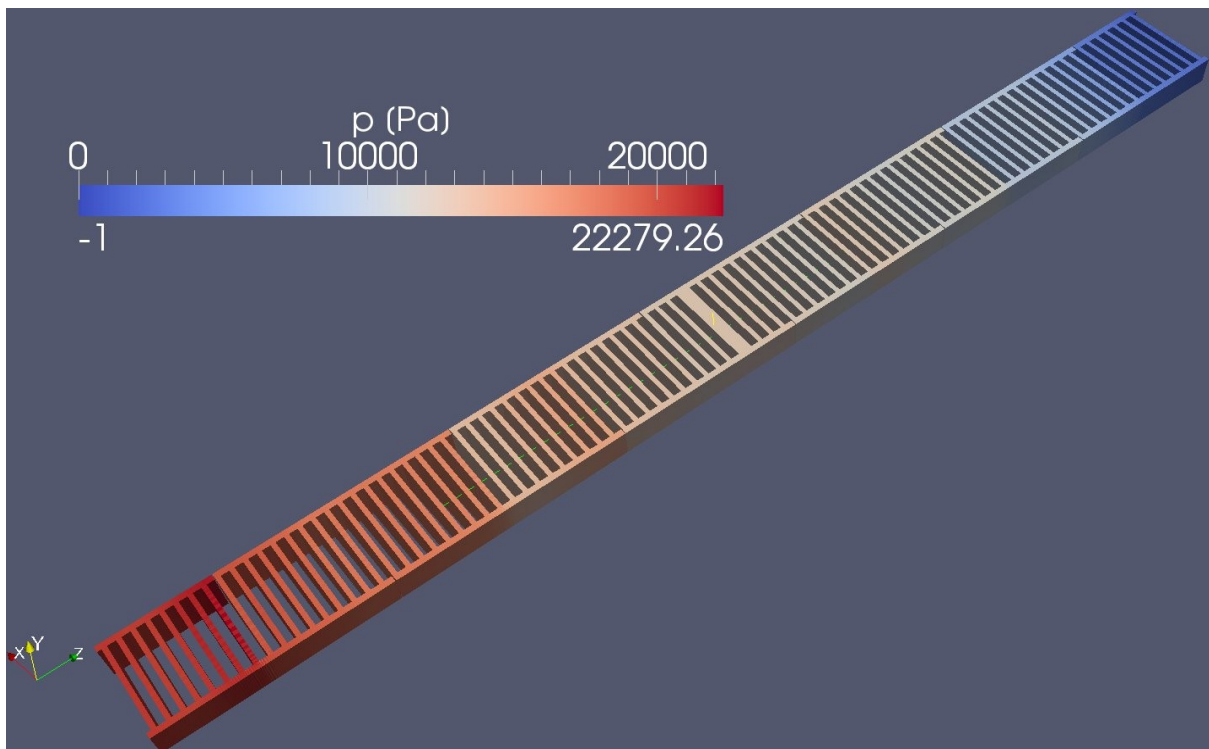


Figure 5 : Pressure of oil in traction transformer winding

The important result of this simulation is the temperature of ester and structural materials shown in the figures below. The temperature steps of the ester at the ester side are caused by the axial pressboard flow barriers. At the spacer side the maximum temperature of the structural materials of 384 K is encountered. For the Nomex 994 this value does not lead to long term stability issues while it may be critical for the pressboard at electrical overload conditions.

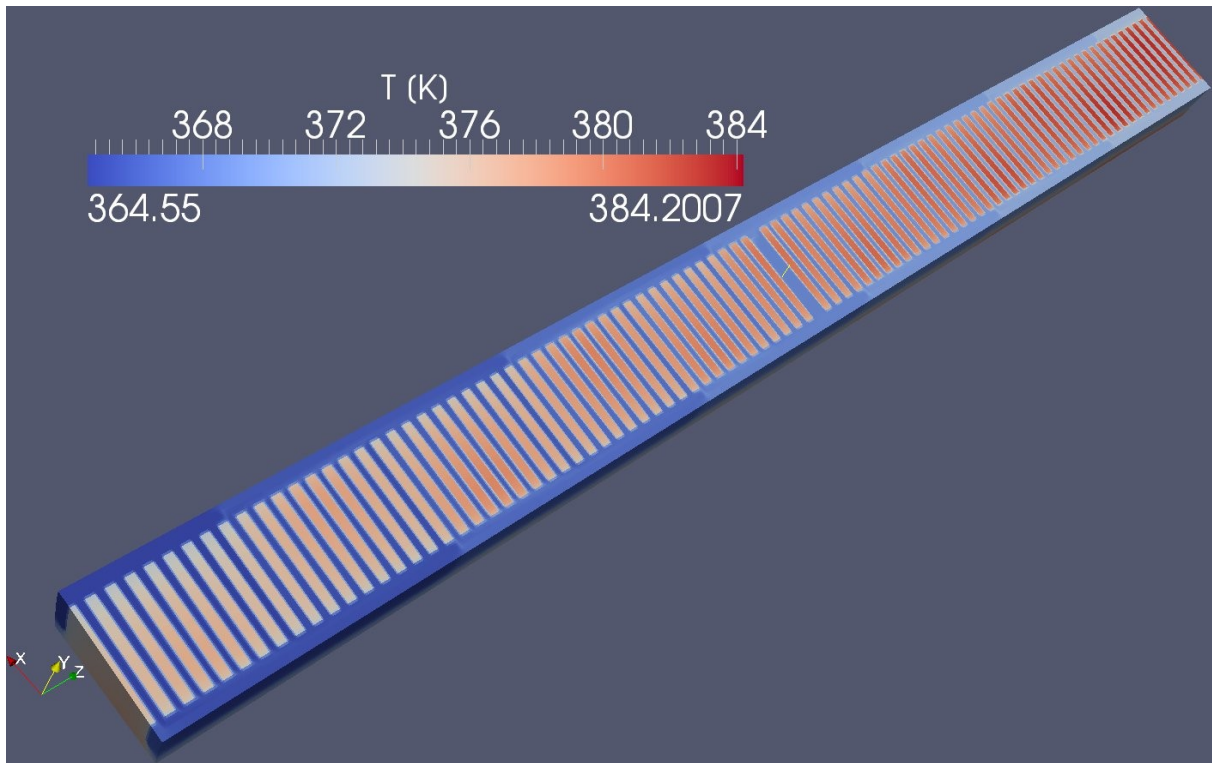


Figure 6 : Temperature of oil and structural materials at ester side in traction transformer winding

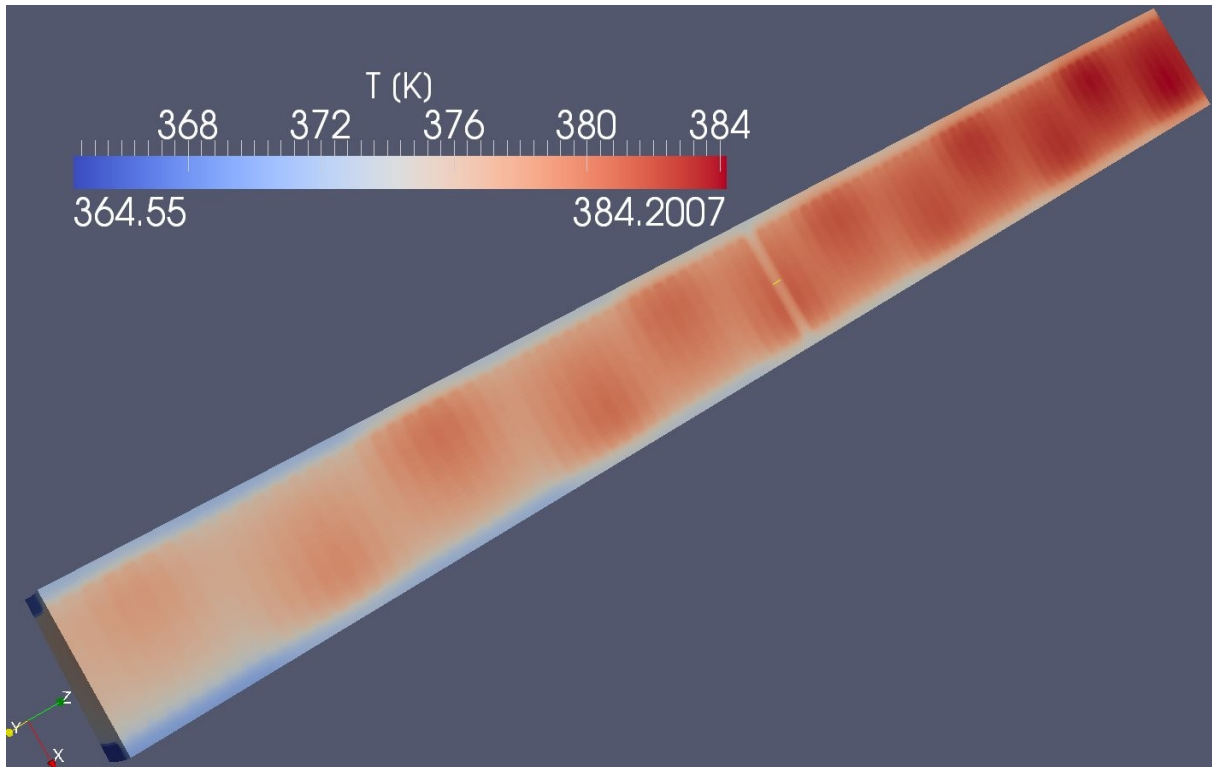


Figure 7 : Temperature of oil and structural materials at spacer side in traction transformer winding

3.2 Cast resin transformer for ships

For a cast resin transformer application we consider an AFWF (Air Forced, Water Forced) transformer operated at ships in an enclosure. The ventilator driven air flow is cooled by pump-driven sea water. An axial air flow barrier inside the enclosure is used to keep the air flow close to the outer side of the HV windings. A set of windings at each of the 3 limbs consists of three LV and one HV windings.

We analyse the core and the windings with prescribed air flow via inlet and outlet boundary conditions imposed by the ventilator. At the entry to the enclosure the air velocity is 4.88 m/s while the air temperature is 300 K.

The following figure provides side and top views of the transformer without enclosure. The right figure shows that between the LV and HV windings there is a thin polyester radiation cylinder. This improves the heat transfer to the air.

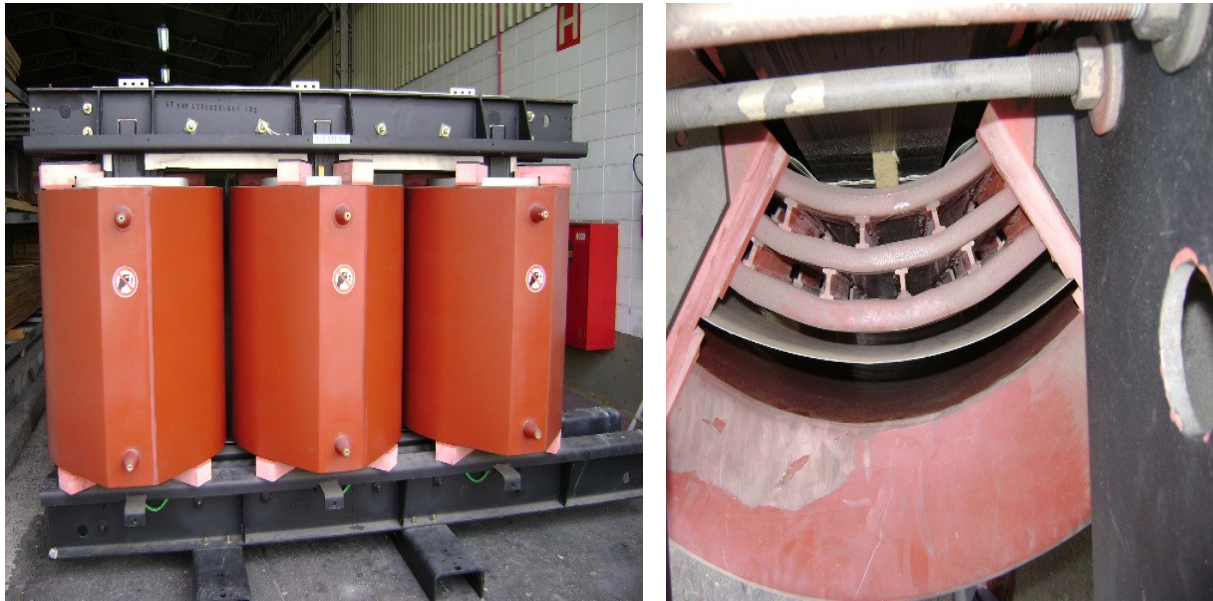


Figure 8a) Side view of cast resin transformer

8b) Top view of windings and radiation cylinder

3.2.1 Material properties

The structural materials considered in this simulation are steel of the core, aluminium of LV and HV windings, cast resin, prepreg, polyester and Cr-Ni-steel of the enclosure. The layers of aluminium conductor and prepreg / polyester insulation are too thin to be resolved in the simulation. However, their vertical layer orientation leads to heat conductivity of 237 W/(m K) in the vertical and 2.2 W/(m K) in the radial direction. To take this into account we use orthotropic heat conductivity in the layers of aluminium and prepreg / polyester in the LV and HV windings.

The structural material properties are considered to be constant while the temperature dependent air properties were taken from [15]. Moreover, in the calculation the radiation emissivities at all surfaces are 0.85.

3.2.2 Simulation results

A key result of the laminar flow simulation is the temperature of air and structural materials shown in the figure below. The winding temperatures are related to local air velocity, radiant heat transfer, and spatial variation of the heat sources. Comparison of the two parts of the figure indicates that the radiation cylinder is quite efficient, since it leads to a significant reduction of the maximum temperature inside the windings.

In the HV windings the lower temperature regions correspond to the cast resin in the surroundings of the layers of aluminium and polyester. The 4 axial steps of the temperature in the HV windings are related to aluminium / polyester regions that are separated by cast resin. The investigated conditions lead to maximum temperatures in the HV windings which are at the upper limit of the class F insulation material.

The figure also shows the upward convection of air heated up at the boundary layers adjacent to core, windings, and radiation cylinder.

At the lower right side of the figures the effect of the axial flow barrier inside the enclosure is visible. It keeps the upward directed air flow close to the outer side of the HV windings. This leads to a step in the axial temperature distribution.

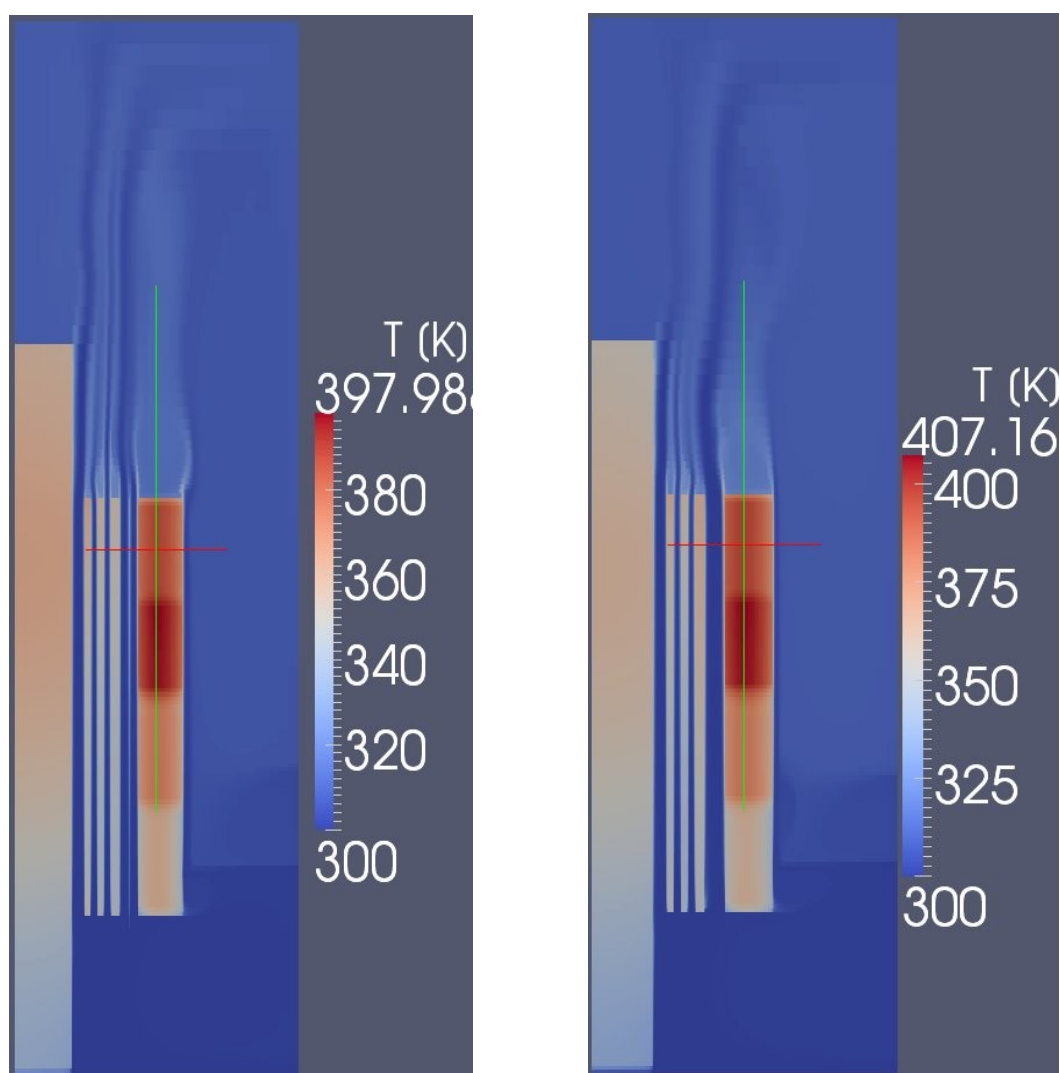


Figure 9a) Temperature with radiation cylinder

9b) Temperature without radiation cylinder

4 SUMMARY AND CONCLUSIONS

The presented results indicate that UniFlow is a useful tool for the thermal design of oil-immersed and dry-type transformers. It can be used to investigate advantages and disadvantages of design features as well as to perform design optimisation.

In addition to the results shown in this paper, the pressure loss encountered in a device as a result of the fluid flow may be a major result of a simulation. This is demonstrated in [13]. Other applications are related to detailed analyses on segments of disc windings with respect to, e.g., modelling of material compositions, width of oil channels, etc.. Another field of application are oil flows in transformer cores. Moreover, combined oil and air flows are analysed in the context of fin type distribution transformers. This is aimed at optimisation of the thermal efficiency of the fins and other tasks. Furthermore, combined oil and air flows in radiators can be investigated.

In addition to steady state analyses, transient processes are investigated. One interesting type of transient occurs at the cold start of a transformer. This matters in particular for oil transformers where the dynamic viscosity is very high at low temperatures, especially for ester fluids.

Due to, e.g., the high voltages, detail measurements inside power transformers are difficult. Nevertheless, the future work will include validation of UniFlow transformer simulations via experiments.

REFERENCES

- [1] Torriano, F., Picher, P., Chaaban, M., *Numerical investigation of 3D flow and thermal effects in a disc-type transformer winding*, Applied Thermal Engineering, 40, pp. 121-131, 2012
- [2] Smolka, J., Nowak, A. J., *Experimental validation of the coupled fluid flow, heat transfer and electromagnetic numerical model of the medium power dry-type electrical transformer*, Int. J. Thermal Sciences, 47, pp. 1393-1410, 2008
- [3] Smolka, J., Biro, O., Nowak, A. J., *Numerical simulation and experimental validation of coupled flow, heat transfer and electromagnetic problems in electrical transformers*, Arch. Comput. Methods Eng, 16, pp. 319-355, 2009
- [4] Fonte, C. M. et. al., *CFD analysis of core type power transformers*, CIRED, 21st intl. Conf. On Electricity distribution, paper. 0361, Frankfurt, 6.-7. 2011
- [5] Gastelurrutia, J. et. al., *Numerical modelling of natural convection of oil inside distribution transformers*, Applied Thermal Engineering, 31, pp. 493-505, 2011
- [6] Landau, L. D., Lifshitz, E. M., *Course of theoretical physics, vol. 6 : Fluid mechanics*, Pergamon Press, Oxford, UK, 1989
- [7] Baehr, H. D., Stephan, K., *Heat and mass transfer*, Springer-Verlag, Berlin, 2006
- [8] Ferziger, J. H., Peric, M., *Computational methods for fluid dynamics*, Springer-Verlag, Berlin, 1999
- [9] van Doormal, J. P., Raithby, G. D., *Enhancements of the SIMPLE method for predicting incompressible flows*, Numer. Heat Transfer, 7, pp. 147-163, 1984
- [10] Issa, R. I., *Solution of implicitly discretized fluid flow equations by operator splitting*, J. Comp. Phys., 62, pp. 40-65, 1986
- [11] Trottenberg, U., Oosterlee, C. W., Schüller, A., *Multigrid*, Academic Press, New York, ISBN 012701070X, 2001
- [12] Notay, Y., *An aggregation-based algebraic multigrid method*, Electronic Transactions on Numerical Analysis, 37, pp. 123-146, Kent State University, ISSN 1068-9613, 2010.
- [13] Tenbohlen, S., Weinklader, A., Wittmaack, R., *Prediction of the oil flow and temperature distribution in power transformers by CFD*, CIGRE Session 2010, Report A2-301, Paris, 2010
- [14] Wittmaack, R., *CFD simulations of oil immersed and dry type transformers*, CIGRE colloquium transformer research, May 16-18, 2012, Dubrovnik, Croatia
- [15] Schlichting, H., *Boundary-layer theory*, McGraw-Hill, New York, USA, 1979